

# Pomeron Weights in QCD Processes at High Energy and the $S$ -Matrix Unitarity Constraint

Rami Oueslati 

*Space sciences, Technologies and Astrophysics Research (STAR) Institute,  
Université de Liège, Bât. B5a, 4000 Liège, Belgium*

(Dated: December 24, 2024)

The pomeron topological cross-section is derived for the eikonal and the  $U$ -matrix unitarization schemes using a generalized expansion of the unitarized elastic amplitude in an effort to examine pomeron characteristics, namely the multiplicity distribution, fluctuation, and correlation, and to reveal the impact of pomeron weights on the  $pp$  multiplicity distribution. The results demonstrate that the  $U$ -matrix inherently incorporates a larger amount of diffraction production into the multi-pomeron vertices, yielding a larger pomerons' variability regardless of the energy range, while such fluctuations become significant only beyond a specific high-energy threshold in the eikonal and quasi-eikonal schemes. Most importantly, our findings indicate that within the  $U$ -matrix scheme, an increase in exchanged pomerons results in more pronounced higher-order pomeron correlations, which are affected by the energy and the impact parameter. Interestingly, our outcomes also highlight that the correlated pomeron exchanges within the  $U$ -matrix summation play a key role in enhancing multi-parton collisions. In light of these results, we can argue that the  $U$ -matrix is fundamentally more valid for theories with growing cross-sections with energy, such as QCD at high energies.

## I. INTRODUCTION

In the study of hadronic interactions at high energy, understanding soft QCD processes that occur at low momentum transfer is a daunting task since perturbative QCD techniques are inapplicable and, to date, there is no fundamental theory that underlies these processes. That being said, we can approach them through phenomenological models that are based on fundamental principles of quantum field theory – such as unitarity, analyticity and crossing symmetry, along with empirical parametrizations. In order to improve these models, extensive data comparisons from collider experiments and cosmic-ray air showers are necessary to validate their underlying assumptions and fine-tune their parameterizations.

One of the most important soft QCD processes is Hadronization, which involves the transformation of quarks and gluons produced in high-energy collisions into the observed hadrons. Indeed, this process has been described by a number of phenomenological models implemented in Monte Carlo event generators. For instance, we can cite the Lund string model [1] in conjunction with the Gribov-Regge theory [2], in Sibyll [3] and QGSJET [4]. In these models, multi-pomeron exchanges play a crucial role in the hadronization process. The unitarization of the elastic scattering amplitude allows for their inclusion, with the eikonal approximation being the most commonly used method satisfying the unitarity principle in this context.

In these models, multi-pomeron exchanges play a crucial role in the hadronization process. The unitarization

of the elastic scattering amplitude allows for their inclusion, with an eikonal-like unitarisation scheme being the most commonly used method satisfying the unitarity principle in this context. Indeed, the formation of string pairs, which corresponds to cut pomerons in the Gribov-Regge framework, is influenced by the weights of the pomerons. These strings, stretched between projectile and target partons, undergo hadronization, leading to the production of observed hadrons. However, despite the reasonable description of some hadronic observables provided by the eikonal or its extended version the quasi-eikonal, both direct and indirect evidence indicate that these approaches are inadequate for a complete understanding of the physics in question, particularly in hadron collisions at (ultra-) high energies. As such, a more comprehensive approach is necessary to accurately describe the complex dynamics involved in these processes.

In [5], it has been shown that pomeron exchange in an eikonal-like scheme is a Poisson-distributed variable, where the number of exchanged pomerons is statistically independent. From a fundamental standpoint, since pomerons are exchanged between composite particles consisting of bound quarks and gluons, there is no sound reason why they should be independent. Hence, it is hypothesized that pomeron exchanges may be correlated and interdependent as a result of interactions between the quarks and gluons. This raises the question of identifying the appropriate unitarization scheme for such dependent exchanges.

From a phenomenological point of view, modelling problems caused by an eikonal-like unitarization technique are numerous. For instance, it has been demonstrated in [6] that shadow corrections to the rapidly rising contribution of the input supercritical pomeron, which arise from pomeron rescatterings or, equivalently, from considering the survival probability factor, do not resolve

---

\* [rami.oueslati@uliege.be](mailto:rami.oueslati@uliege.be)

the Finkelstein-Kajantie problem. Consequently, it has been argued that an alternative method for unitarization is necessary.

Another fundamental issue that needs to be addressed relates to string models for hadronization [7]. In these models, the probability of configurations with  $n$  string pairs is given by the probability of having  $n$  exchanged pomerons, which is a Poisson distribution through the eikonal scheme. Nevertheless, this approach is inconsistent for the following reasons.

To begin with, in the string model, the first pair of quark-antiquark strings and the subsequent pairs are fundamentally different. This distinction arises because the first string pair is formed from the initial quarks of the colliding protons, while the subsequent pairs are typically generated from secondary interactions. These secondary interactions involve different quark content and a different distribution of energy among the strings, with the first string pair generally receiving a larger share of the available energy compared to the subsequent pairs. Conversely, in the Gribov-Regge theory, all elementary interactions -pomerons- are treated as identical. Thus there is no distinction between the initial and subsequent interactions and all pomerons are dealt with statistically uniformly. Additionally, in the Gribov-Regge framework, the energy sharing among the different pomerons is not considered. These inconsistencies result in a mismatch when using the Gribov-Regge pomeron probability distribution for configurations with different numbers of string pairs. Therefore, we can argue that this mismatch is attributed to the eikonal scheme given that the Gribov-Regge pomeron probability is essentially Poissonian and basically defined from the eikonal scheme. Consequently, considering an alternative unitarisation scheme, namely the  $U$ -matrix, could be a solution to the aforementioned issues. In fact, throughout the years, various arguments have been furnished in favor of the  $U$ -matrix scheme.

For instance, in [8], a phenomenological model based on the picture depicting the KNO scaling violation as an extension of the geometrical scaling violation and using the  $U$ -matrix unitarization scheme has been presented within the framework of the geometrical approach in an attempt to describe multi-particle production. In this study, it has been suggested that the  $U$ -matrix scheme may serve as a noteworthy alternative for tackling challenges related to multi-particle production in hadron collisions, especially in scenarios where extreme conditions and rare events play a significant role in high and ultra-high energy physics. It also prompts an inquiry into the fundamental nature of pomeron exchange within the  $U$ -matrix scheme in comparison to the eikonal, despite that both schemes verify the unitarity constraint principle.

In another study [9], owing to the fact that correlations could arise from hadron fluctuations in various diffractive configurations, a multi-channel model was introduced to better describe diffractive cross-sections by enhancing these hadron fluctuations. This model has shown that  $U$ -matrix unitarization is likely incompatible

with the assumption of uncorrelated pomeron exchange, primarily because the findings are independent of the details of the diffractive states.

In addition, the rational form of unitarization (e.g., the  $U$ -matrix) has long been supported by arguments based on the analytical features of the scattering amplitude. It has been demonstrated that, in contrast to the exponential form of unitarization (e.g., the eikonal), this type of unitarization far more easily replicates correct analytical characteristics of the amplitude in the complex energy plane [10]. Moreover, much research (e.g., [8, 11]) has highlighted the efficacy of the rational form in offering a more accurate description of the underlying physics in hadronic collisions at high energy.

At ultra-high energy, it has been shown that the eikonal causes problems in describing the data obtained from cosmic-ray air showers. Indeed, the development of air showers can be significantly affected by diffractive collisions [12]. For example, based on the predictions of MC simulations, it has been revealed that diffractive collisions have an impact on the prediction of observables in ultra-high energy cosmic ray experiments, such as the depth of the maximum of the shower development  $X_{max}$  and the depth of the maximum of the muon productions in an air shower  $X_{max}^\mu$ . As it has been revealed in [13] the single diffractive data preferred the  $U$ -matrix scheme over the eikonal, particularly at ultra-high energy. Switching from the commonly used eikonal in these MC simulations could hence reshape our understanding of cosmic-ray physics.

Overall, selecting the appropriate elastic scattering amplitude unitarisation is primordial in high-energy hadron scattering, particularly for various phenomenological models and generators. Indeed, multi-pomeron exchange weights considerably impact high-energy hadron amplitudes, thereby directly affecting hadron process cross-sections. This includes the energy-dependent growth pattern of inclusive cross-sections and the shape of produced particle multiplicity distributions [14, 15].

The study set out to understand the nature and role of pomeron exchanges in the  $U$ -matrix scheme in comparison to an eikonal-like one. It also aims to shed light on the impact of the pomeron weights for QCD processes.

This work is organized as follows. In the next section, we will outline the theoretical framework of the pomeron vertices in Gribov-Regge theory, along with a detailed review of the generalized representation of the unitarized elastic scattering amplitude, as proposed by Kancheli. Section III will present and thoroughly discuss the results. Section IV will summarize the main findings and implications of the study.

## II. POMERONS VERTICES IN GRIBOV-REGGE THEORY

Unitarization in the Gribov-Regge theory [2] is accomplished by summing the contributions from all multi-reggeon exchanges. Using this method, the Reggeon vertices, referring to the coupling between the exchanged Reggeons and the external particle, are used to calculate the amplitudes for multi-Reggeon exchanges and their values determine the weights of the n-reggeon exchange. It is worth noting that it is difficult to compute the values of these vertices from first principles. In fact, from a phenomenological procedure, they are parameters determined by fitting to experimental data using some functional form. However, as previously stated in the first section, there is no specific reason to assume that these weights should adhere to the simple Glauber-eikonal form. Therefore, a more thorough treatment of them is needed. In [16], the structure of these multi-pomeron vertices has been analyzed and generalized to take into account more complex interactions, specifically the contribution from diffraction production in the weights of multi-reggeon exchange. In this section, the formalism put forth in [16] will be thoroughly reviewed as it lies the theoretical foundations for our objectives.

We begin with the expression of the unitarized elastic hadronic amplitude represented as follows :

$$F(s, t) = \sum_{n=1}^{\infty} F_n(s, t), \quad (1)$$

with the  $n$  Reggeon exchange amplitude given by :

$$F_n(s, t \simeq -k_{\perp}^2) = \frac{-i}{nn!} \int N_n^2(k_{\perp i}) \cdot \prod_{i=1}^n \frac{d^2 k_{\perp i}}{(2\pi)^2} \cdot D(s, k_{\perp i}) \delta^2 \left( k_{\perp} - \sum k_{\perp i} \right), \quad (2)$$

where at high energy, the primary amplitude  $F_1(s, t)$  can be represented either as a pomeron exchange or as a more intricate set of reggeon diagrams and its factorized form

$$N_n(k_i) = \sum_{\nu_1, \dots, \nu_{n-1}} \langle P_{in} | \hat{G}(k_1) | \nu_1 \rangle \langle \nu_1 | \hat{G}(k_2) | \nu_2 \rangle \langle \nu_2 | \hat{G}(k_3) | \nu_3 \rangle \cdots \langle \nu_{n-2} | \hat{G}(k_{n-1}) | \nu_{n-1} \rangle \langle \nu_{n-1} | \hat{G}(k_n) | P_{out} \rangle \quad (6)$$

One can simplify the handling of the vertex operators  $\hat{G}(k)$  by redefining the basis for the beam states  $|\nu\rangle$  where  $\hat{G}(k)$  has a simple diagonal form :

$$\hat{G}(k)|\nu\rangle = g_{\nu}(k)|\nu\rangle, \quad (7)$$

is given by

$$F_1(s, t) = G(k_{\perp})D(s, k_{\perp})G(k_{\perp}), \quad (3)$$

where  $D(s, k_{\perp})$  refers to the Green function of the Pomeron. As stated in [17], the vertex function  $N_n(k_{\perp i})$  in (2), representing the emission of  $n$  pomerons with transverse momenta  $k_{\perp i}$  by the external hadron particle, can be expressed through integrals of the product of  $G$  vertices. Likewise, the vertices can be expanded over on mass shell states of diffractive-like beams [18], thereby accounting for the contribution from diffractive production in the multi-reggeon exchange weights :

$$N_n(k_i) = \sum_{\nu_1, \nu_2, \dots, \nu_n} \int G_{1 \nu_1}(P_{in}, p_i^{(1)}) G_{\nu_1 \nu_2}(p_i^{(1)}, p_j^{(2)}) \cdots \cdots G_{\nu_{n-1} 1}(p_i^{(n-1)}, P_{out}) \prod_{i=1}^{n-1} d\Omega_{\nu_i}(p_i^{(1)}), \quad (4)$$

where  $G_{\nu_1 \nu_2}(p_i^{(1)}, p_j^{(2)}, k_{\perp})$  is the transition amplitude for a beam of  $\nu_1$  particles with momenta  $p_i^{(1)}$  into a beam of  $\nu_2$  particles with momenta  $p_j^{(2)}$ , and with the emission of a pomeron with the transverse momentum  $k_{\perp}$ . In (4), the  $d\Omega_{\nu}(p_i)$  represents the element of the  $\nu$  particles phase-space volume. The Eq. (4) incorporates both the summation and integration over all conceivable physical states of the particles in the beams and thus accounts for their full masses. It is important to note that the multi-particle amplitudes  $G_{\nu_1 \nu_2}$  are complex and may contain unrelated contributions, whereas the vertex functions  $N_n(k_i)$  are real.

Considering a non-local field operator  $\hat{G}(k)$  describing the pomeron emission vertices  $G_{\nu_1 \nu_2}(k)$  between the initial and final states of the external particle, the expression (4) for the vertex functions  $N_n(k_i)$  can be written in a symbolic operator form as the average of the product of this field operator  $\hat{G}(k)$  :

$$N_n(k_i) = \langle P_{in} | \hat{G}(k_1) \hat{G}(k_2) \cdots \hat{G}(k_n) | P_{out} \rangle \quad (5)$$

This product can further be decomposed over the complete set of physical states of the beams  $|\nu\rangle$  as follows

with  $g_{\nu}(k)$  acting as eigenvalues. Then the expression Eq. (6) is simplified as the summation over all possible beam states, with the contribution from each state weighted by a function  $w(\nu)$  and the product of its associated vertex functions for the different momentum com-

ponents  $k_i$  :

$$N_n(k_i) = \sum_{\nu} w(\nu) \prod_1^n g_{\nu}(k_i) \quad (8)$$

where  $w(\nu)$  can be interpreted as the probability of finding the fast hadron in the state  $|\nu\rangle$  and is given by:

$$w(\nu) = \langle P_{in}|\nu\rangle \langle \nu|P_{out}\rangle \quad (9)$$

Following this simplification, the  $S$ -matrix in the impact parameter representation can be written as follows:

$$\begin{aligned} S(s, b) &= \sum_{\nu_1 \nu_2} w(\nu_1) w(\nu_2) \sum_{n=0}^{\infty} \frac{(i \chi_{\nu_1 \nu_2}(s, b))^n}{n!} \quad (10) \\ &= \sum_{\nu_1 \nu_2} w(\nu_1) w(\nu_2) e^{i \chi_{\nu_1 \nu_2}(s, b)} \end{aligned}$$

where

$$\chi_{\nu_1 \nu_2}(s, b) = \int d^2 k_{\perp} e^{i b k_{\perp}} g_{\nu_1}(k_{\perp}) D(s, k_{\perp}) g_{\nu_2}(k_{\perp}) \quad (11)$$

One can further simplify the expression for the vertices by factorizing the vertex function  $g_{\nu}(k)$  into a universal term  $g(k)$  and a state-dependent coefficient  $\lambda(\nu)$ , with a small non-factorizable correction  $\tilde{g}(\nu, k)$  :

$$g_{\nu}(k) = g(k) \lambda(\nu) + \tilde{g}(\nu, k) \quad (12)$$

then the vertices can be represented as :

$$N_n(k_i) \simeq \beta_n \prod_1^n g(k_i), \quad (13)$$

where

$$\beta_n = \sum_{\nu} w(\nu) (\lambda(\nu))^n \quad (14)$$

Under this assumption of factorization, the vertices simplify to a product of universal functions  $g(k_i)$ , weighted by  $\beta_n$ , which encapsulates the sum over the probabilities  $w(\nu)$  and the coefficients  $(\lambda(\nu))^n$ .

All in all we obtain the following expression for the  $S$ -Matrix in the impact parameter representation :

$$S(s, b) = \sum_{n=0}^{\infty} \frac{\beta_n^2}{n!} (i \chi(s, b))^n \quad (15)$$

where the real coefficients  $\beta_n \geq 1$  are largely arbitrary. Yet, their expressions will be determined depending on the unitarisation scheme chosen for the elastic amplitude, which will be illustrated in the forthcoming section.

The above equation provides a generalized expansion of the  $S$ -matrix whereby the coefficients govern the contributions of different orders of the interaction between the particles. Technically, the expansion is developed as

a power series increasingly summing over complex interaction terms dictated by the function  $\chi(s, b)$  which incorporates the scattering dynamics. Each term's weight is controlled by the coefficient  $\beta_n$ , reflecting the relative probability of different interaction strengths leading to the scattering process.

It is often not feasible to work directly with an infinite series due to the computational cost of calculating each term and the potential difficulty of evaluating the convergence characteristics. Yet, it might be possible to gain a better understanding of the series' structure in (38) by constructing a more compact and manageable formulation. This can be accomplished in a few different ways, for instance by mapping the series into an integral. By using spectral theory, for example, hidden spectral properties may be uncovered. To do so, we replace the coefficients  $\beta_n$  in (38) with the following expression :

$$\beta_n = \int_0^{\infty} d\tau \tau^n \varphi(\tau), \quad (16)$$

then the  $S[\chi]$  matrix can be rewritten as a combination of Glauber-type eikonal terms:

$$S(s, b) \equiv S[\chi] = \int_0^{\infty} d\tau \rho(\tau) e^{i\tau\chi(s, b)} \quad (17)$$

$$\rho(\tau) = \int_0^{\infty} \frac{d\tau_1}{\tau_1} \varphi(\tau_1) \varphi(\tau/\tau_1) \quad (18)$$

where  $\rho(\tau)$  functions as a weight. The constraints  $\beta_0 = \beta_1 = 1$  are imposed by the normalization condition for  $S[\chi]$  and  $w(\nu)$ . This results in the following relations:

$$\int_0^{\infty} d\tau \rho(\tau) = \int_0^{\infty} d\tau \tau \rho(\tau) = 1 \quad (19)$$

It is worth noting that, in the Glauber eikonal case, the single-particle state in beams contributes very little to  $N_n(k_i)$ . When this occurs, the integrals in (4) disappear and the expression for  $N_n(k_i)$  becomes a simple product of  $n$  elastic pomeron vertices as :

$$N_n(k_i) = \prod_{i=1}^n g(k_i), \quad (20)$$

where  $g(k) = G_{11}(p, p+k)$ .

Using the generalised  $S$  matrix representation, we can write some general relationships for cross-sections at a given impact parameter, which are expressed using the function  $S[\chi(s, b)]$ , and are valid for any spectral density  $\rho(\tau)$ .

- The total cross-section :

$$\sigma_{tot}(s, b) = 2(1 - Re(S[\chi])), \quad (21)$$

- The elastic cross-section

$$\sigma_{el}(s, b) = |1 - S[\chi]|^2, \quad (22)$$

- The total inelastic cross-section

$$\sigma_{in}(s, b) = \sigma_{tot} - \sigma_{el} = 1 - |S[\chi]|^2 \quad (23)$$

- The total cross-section of diffraction generation : single  $\sigma_{sd}$  and double  $\sigma_{dd}$

$$\begin{aligned} \sigma_{dif}(s, b) &= \sigma_{in} - \sigma_{in, cut} = 2\sigma_{sd} + \sigma_{dd} \\ &= S[2i\text{Im}(\chi)] - |S[\chi]|^2 \end{aligned} \quad (24)$$

- The cross-section corresponding to processes when at least one pomeron is s-cut : when we cut a single pomeron from the elastic amplitude, this corresponds to taking the imaginary part of the corresponding partial-wave amplitude. From the optical theorem, we know that this is related to the cross-section for cutting a single pomeron. Therefore

$$\sigma_{in, cut}(s, b) = 1 - S[2i\text{Im}(\chi)] \quad (25)$$

and so the pomeron topological cross-section: these are the contributions of diagrams with  $n$  cut pomerons and of the arbitrary number of uncut pomeron lines

$$\sigma_n(s, b) = \int_0^\infty d\tau \rho(\tau) \frac{(2\tau\text{Im}(\chi))^n}{n!} e^{-2\tau\text{Im}(\chi)} \quad (26)$$

where  $\rho(\tau)$  is a spectral density. The pomeron topological cross-section resembles a superposition of Poisson distributions, where each term represents the contribution of a Poisson distribution with mean  $(2\tau\text{Im}(\chi))$  weighted by the spectral density  $\rho(\tau)$ .

### III. RESULTS

#### A. Pomeron topological cross-section

This section is concerned with the investigation of the pomeron dynamics by utilizing the general representation of the  $S$ -Matrix. First of all, we start with highlighting the link between this general representation and the unitarization scheme and then with the pomeron weights. Let's examine two prominent unitarization schemes: the eikonal and the  $U$ -matrix. They are distinguished by

their respective spectral functions  $\rho(\tau)$ , i.e. the  $\beta_n$  coefficients. For instance, if we consider a simple spectral function as a delta function,

$$\rho(\tau) = \delta(\tau - 1), \quad (27)$$

then we obtain for the unitarised elastic scattering amplitude, the following expression :

$$A(s, b) = i \left[ 1 - e^{i\chi(s, b)} \right] \quad (28)$$

which is the eikonal form of the unitarisation scheme [19]. In this case, using Eq. 26, the pomeron topological cross-section is given by

$$\sigma_n(s, b) = \frac{(2\text{Im}(\chi))^n}{n!} e^{-2\text{Im}(\chi)} \quad (29)$$

While if we take for the spectral function, the expression :

$$\rho(\tau) = \frac{e^{-\tau/c}}{c} \quad (30)$$

[20] and with  $c = \frac{1}{2}$  then we get for the unitarised elastic scattering amplitude, this form :

$$A(s, b) = \frac{\chi(s, b)}{1 - i\chi(s, b)/2} \quad (31)$$

which is the  $U$ -Matrix form of the unitarisation scheme [19], and for the pomeron topological cross-section, Eq. 26 gives :

$$\sigma_n(s, b) = \frac{(\text{Im}(\chi))^n}{(1 + \text{Im}(\chi))^{1+n}} \quad (32)$$

It is worth noting that different schemes for unitarizing the elastic amplitude, and hence various approaches to ensure the unitarity constraint, arise from the generalized  $S$  matrix form, which depends on the choice of the spectral function. Owing to the ambiguity of selecting the appropriate unitarisation scheme, particularly for hadron scattering at high energy, in spite of satisfying the unitarity constraint, one can resort to some general procedure. Indeed, it is significant to note that the optimization of a phenomenological model from the general expansion of the  $S$ -matrix may facilitate the identification of the suitable scheme. This can be achieved by fitting experimental data to some observables, such as total, elastic and inelastic cross-sections, among others. Then, the adequate scheme can be determined by deriving the appropriate spectral function from the best fits.

In the eikonal case, the number of pomerons is a random variable Poisson distributed [5]. Therefore, one may inquire about the nature of the probability distribution for the number of pomeron exchanged in alternative approaches, mainly the  $U$ -matrix scheme. As a matter of

fact, the expression 26 of the pomeron topological cross-section  $\sigma_n(s, b)$ , as a superposition of Poisson distribution, can be understood as a mixed Poisson distribution, in which the conditional distribution of the number of pomeron exchanged, given a certain rate parameter, is a Poisson distribution. Nevertheless, the rate parameter itself, in the mixed poisson framework, is handled as a random variable with its own distribution [21]. Thus, one can query what kind of features can be obtained with this random rate parameter rather than with a fixed Poisson rate parameter for all events. To achieve this, let a

random variable  $X$  satisfies a mixed Poisson distribution with density  $\pi(\lambda)$ , then the probability distribution has this form :

$$Pr(X = n) = \int_0^\infty \frac{\lambda^n}{n!} e^{-\lambda} \pi(\lambda) d\lambda. \quad (33)$$

If we consider that the Poisson rate parameter is distributed according to an exponential distribution,  $\pi(\lambda) = \frac{1}{\gamma} e^{-\frac{\lambda}{\gamma}}$  and using integration by parts  $n$  times yields:

$$Pr(X = n) = \frac{1}{n!} \int_0^\infty \lambda^n e^{-\lambda} \frac{1}{\gamma} e^{-\frac{\lambda}{\gamma}} d\lambda = \left( \frac{\gamma}{1+\gamma} \right)^n \left( \frac{1}{1+\gamma} \right) \quad (34)$$

we get  $X \sim \text{Geo}\left(\frac{1}{1+\gamma}\right)$ . And so the pomeron probability distribution in case of the  $U$ -matrix scheme gives the probability distribution of the number of failures until the first success of the exchanged pomerons.

$$Pr(X = n) = (1-p)^n p \quad (35)$$

for  $n = 0, 1, 2, 3, \dots$ , where

$$p = \frac{1}{1+\gamma} \quad (36)$$

Thus, when compounding a Poisson distribution with rate parameter distributed according to an exponential distribution yields a geometric distribution. Or according to (32), for the pomeron topological cross-section in the  $U$ -Matrix case, we have :

$$P(X = n) = \left( \frac{\gamma}{1+\gamma} \right)^n \left( \frac{1}{1+\gamma} \right) = \sigma_n(s, b) = \frac{(\text{Im}(\chi(s, b)))^n}{(1 + \text{Im}(\chi(s, b)))^{1+n}}, \quad (37)$$

with  $\gamma = \text{Im}(\chi(s, b))$ . Consequently, within the  $U$ -matrix scheme, the number of pomerons is a random variable that follows a geometric distribution, and hence pomeron exchanges are no longer independent, and this dependency implies collective phenomena such as correlation among the exchanged pomerons. This outcome distinguishes the  $U$ -matrix scheme from others, particularly the eikonal, which lacks these properties.

Another approach in [22] involves deriving the pomeron topological cross-section by applying the AGK cutting rules and using the coefficients obtained in each scheme by expanding the elastic scattering amplitude in impact parameter space as a power series of the Born term. The resulting expression is very similar to our result 32, with the main difference being an additional multiplicative factor of 2. Moreover, it was shown that the  $U$ -matrix unitarization is inconsistent with the AGK rules and in turn that the  $U$ -matrix scheme cannot be used for the unitarization of the pomeron with intercept greater than 1. Nevertheless, using the generalized

representation of the  $S$  matrix 38, and the constraints  $\beta_0 = 1$  imposed by the normalization condition for  $S[\chi]$  and  $w(\nu)$  :

$$S(s, b) = \beta_0^2 + \sum_{n=1}^{\infty} \frac{\beta_n^2}{n!} (i \chi(s, b))^n = 1 + i A(s, b) \quad (38)$$

we obtain a generalized expansion of the unitarized elastic amplitude in impact parameter space :

$$A(s, b) = -i \sum_{n=1}^{\infty} \frac{\beta_n^2}{n!} (i \chi(s, b))^n \quad (39)$$

To obtain the expression of the unitarized elastic amplitude in each scheme, fixing in 39, the weight's coefficient  $\beta_n^2$ , reflecting the relative probability of different interaction strengths.

For the eikonal, case, let  $\beta_n^2 = 1$  and so (39) implies

$$A(s, b) = i[1 - e^{i\chi(s, b)}] = -i \sum_{n=1}^{\infty} \frac{[i\chi(s, b)]^n}{n!} = i \sum_{n=1}^{\infty} C_n^{eik} \cdot (-1)^{n-1} [\Omega(s, b)]^n, \quad (40)$$

where  $\Omega(s, b) \equiv -2i\chi(s, b)$  is the opacity of  $pp$  interaction, and the coefficients of the power series are as in [22]:

$$C_n^{eik} = 2^{-n}/n!, \quad (41)$$

and for the  $U$ -matrix case, let  $\beta_n^2 = c^n/n!$  [23] with  $c = \frac{1}{2}$ , then (39) gives

$$\mathcal{A}(s, b) = \frac{\hat{\chi}(s, b)}{1 - i\hat{\chi}(s, b)/2} = -2i \sum_{n=1}^{\infty} \frac{[i\hat{\chi}(s, b)]^n}{2^n} = i \sum_{n=1}^{\infty} C_n^U \cdot (-1)^{n-1} [\hat{\Omega}(s, b)]^n, \quad (42)$$

where  $\hat{\Omega}(s, b) \equiv -2i\hat{\chi}(s, b)$  is the respective opacity, and the coefficients of the power series are :

$$C_n^U = 1/4^n \quad (43)$$

Note that, as opposed to [22], the first two terms of the pomeron exchange in the eikonal (40) and the  $U$ -matrix (42) schemes (with  $\Omega = \mathbb{P} = \hat{\Omega}$ ) are not the same. Using the expression from [22] of the pomeron topological cross-section derived by applying the AGK cutting rules :

$$\sigma^k(s, b) = 2 \sum_n C_n \cdot (-1)^{n-k} 2^{n-1} \frac{n! [\mathbb{P}(s, b)]^n}{k!(n-k)!}. \quad (44)$$

and replacing in (44) the coefficients  $C_n$  by  $C_n^U$  in the  $U$  matrix case, we get

$$\sigma_U^k(s, b) = \left[ \frac{\text{Im}\hat{\chi}(s, b)}{1 + \text{Im}\hat{\chi}(s, b)} \right]^k \frac{1}{1 + \text{Im}\hat{\chi}(s, b)} \quad (45)$$

exactly the same as our result (32). Regarding the problem of the inconsistency of the  $U$ -matrix unitarization with the AGK rules, we have from the unitarity equation in impact parameter space and (42) that:

$$\begin{aligned} G_{inel}(s, b) &= 2\text{Im}\mathcal{A}(s, b) - |\mathcal{A}(s, b)|^2 \\ &= \frac{2\text{Im}\hat{\chi}(s, b)}{(1 - i\hat{\chi}(s, b)/2)(1 + i\hat{\chi}^*(s, b)/2)}, \end{aligned} \quad (46)$$

and from (45) we get

$$G_{inel}(s, b) = \sum_k \sigma_U^k(s, b) = \frac{\text{Im}\hat{\chi}(s, b)}{1 + \text{Im}\hat{\chi}(s, b)}. \quad (47)$$

In particular, at very large  $s \rightarrow \infty$  according to (46)  $G_{inel} \rightarrow 0$  whereas from (47)  $G_{inel} \rightarrow 1$ . It is worth noting that the limit  $G_{inel} \rightarrow 1$  provides a more physically consistent approximation of inelastic scattering at

large  $\hat{\chi}$ , as it better reflects the suppression of contributions compared to the unphysical saturation implied by  $G_{inel} \rightarrow 2$  in [22], bringing it closer to the expected asymptotic behavior of  $G_{inel} \rightarrow 0$ . Moreover, the discrepancy between the limit of convergence of  $G_{inel}$  in our result and the physical limit of convergence arises from the fact that, in the application of the AGK cutting rules in [22], the cut amplitude does not include contributions from the cross-section of the diffractive states, which corresponds to the production of states accompanied by a rapidity gap. Indeed, the AGK cutting rules relate different cuts of the same diagram, potentially leading to subtle connections or cancellations.

## B. Pomeron multiplicity distribution

Let us quantify the implications of this finding in an explicit model. The starting point is the single pomeron scattering amplitude, i.e. the Born term. We parameterise it as

$$a(s, t) = g_p^2 F_1(t)^2 \left( \frac{s}{s_0} \right)^{\alpha(t)} \xi(t), \quad (48)$$

using the pomeron trajectory  $\alpha(t)$ , the proton elastic form factor  $F_1(t)$  and the coupling pomeron-proton  $g_p$ , with  $\xi(t)$  the signature factor

$$\xi(t) = -e^{-\frac{i\pi\alpha(t)}{2}}. \quad (49)$$

and the pomeron trajectory close to a straight line

$$\alpha(t) = 1 + \epsilon + \alpha't. \quad (50)$$

In the impact-parameter representation, where the Fourier transform of the amplitude  $a(s, t)$  rescaled by  $2s$  is equivalent to a partial wave

$$\chi(s, \mathbf{b}) = \int \frac{d^2\mathbf{q}}{(2\pi)^2} \frac{a(s, t)}{2s} e^{i\mathbf{q}\cdot\mathbf{b}}. \quad (51)$$

We used a dipole-like form factor for the proton  $F_1 = 1/(1 - t/t_0)^2$ . The parameters  $\epsilon$  and  $\alpha'$  describing the pomeron trajectory, the coupling constant  $g_p$  and  $t_0$  the form-factor scale, are adjusted from a fit to up-to-date hadron collider data on total, elastic and inelastic cross-sections both for the eikonal and  $U$ -matrix unitarisation schemes [24] and are provided in table I.

In order to understand the hadronic dynamics at high and ultra-high energies, particularly in terms of the spatial distribution of the interactions and their implications for particle production, we examined the behaviour of the pomeron topological cross-section in the impact parameter space with energy and the number of pomerons exchanged, in both the eikonal and  $U$ -matrix cases, as shown in Fig. 1 and Fig. 2.

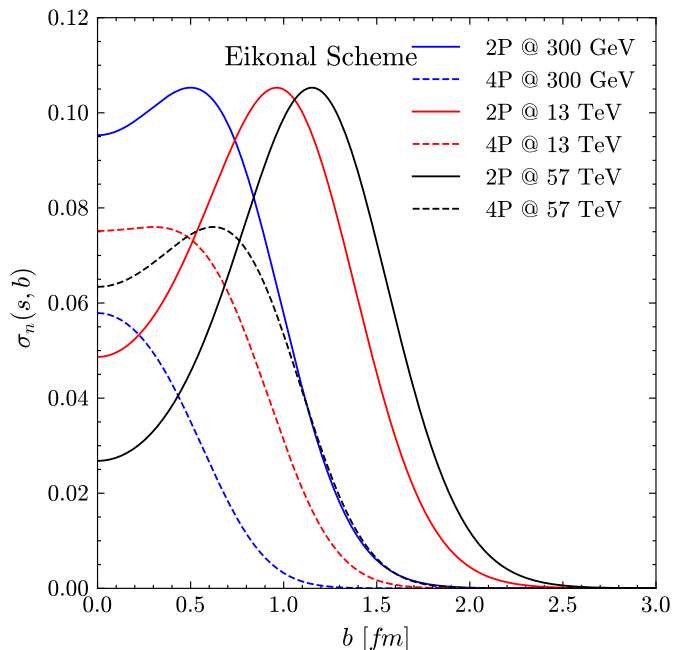


FIG. 1. Impact parameter evolution of the Pomeron Topological cross-section in the Eikonal case.

As can be seen from both figures, this function exhibits a distinct pattern in impact parameter space regardless of the scheme used. Nevertheless in each scheme, it has a broadly similar shape irrespective of both the energy level and the number of the pomerons exchanged. More specifically, as shown in the eikonal case, this function is predominantly peripheral, indicating a substantial contribution at large impact parameters. This implies that the majority of pomeron interactions are more likely to occur when the colliding hadrons pass through each other at large distances, reflecting that the interactions are "softer" in nature, meaning they involve long-range processes, likely mediated by soft pomeron exchanges. On the other hand, in the  $U$  matrix case, we can clearly see that this function is primarily central, suggesting that pomeron interactions tend to happen when the colliding hadrons pass through each other in close proximity, en-

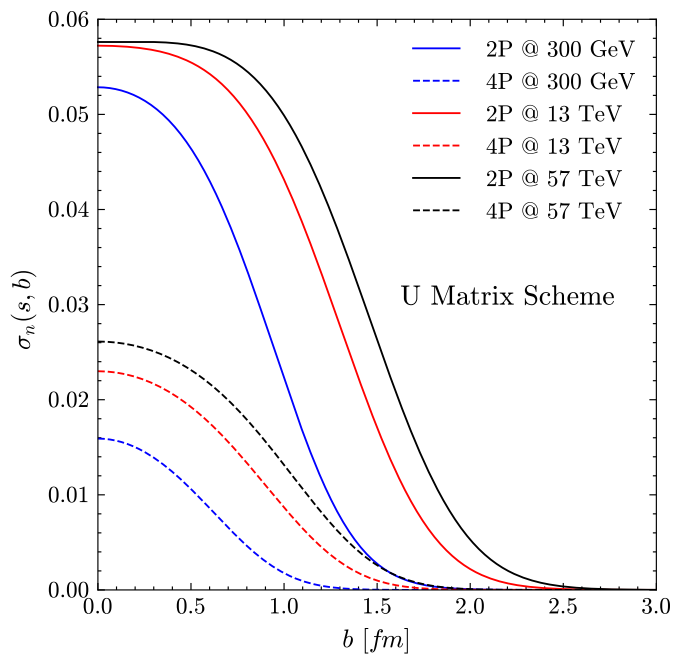


FIG. 2. Impact parameter evolution of the Pomeron Topological cross-section in the  $U$ -Matrix case.

tailing that the collisions tend to involve higher energy densities, leading to more intense interactions in the core of the colliding hadrons.

Furthermore, another aspect observed from these figures is that, with the exponential scheme, this function tends to decline in the same manner with respect to the impact parameter as energy increases. Notably, for a given  $n$ , the peak of this function shifts toward larger values of  $b$  with increasing energy, while the magnitude of the peak remains approximately constant. This suggests that the spatial region, where the interactions take place, expands with increasing energy, making peripheral collisions even more dominant at ultra-high energy. Most importantly, this peripheral behaviour and constancy of the peak's magnitude are indicative of reaching a saturation effect where the available parton density limits the increase in the interaction strength even with increasing energy.

Whereas, with the rational scheme, this cross-section typically shows a more gradual decrease with increasing impact parameter as energy rises. More interestingly, for a given  $n$ , the maximum remains near the centre of the collision, and its value increases with energy. This indicates that the strength of the pomeron interactions grows at the core of the collision and we can understand that more partons are involved in the interaction in the central region. This reflects a regime where the interactions are still increasing, indicating that saturation has not yet been reached in the central collision region.

Additionally, according to these figures, it is clear that, for a fixed energy, with two and four pomerons exchanged the magnitude of this function decreases as  $n$  increases



Scheme	$\epsilon$	$\alpha'$	$g_p$	$t_0$	$\frac{\chi^2}{\text{d.o.f}}$
Eikonal	$0.11 \pm 0.01$	$0.31 \pm 0.19$	$7.3 \pm 0.9$	$1.9 \pm 0.4$	1.442
U-matrix	$0.10 \pm 0.01$	$0.37 \pm 0.28$	$7.5 \pm 0.8$	$2.5 \pm 0.6$	1.436

TABLE I.  $\chi^2/\text{d.o.f}$  and best-fit parameters obtained using the eikonal and  $U$ -matrix unitarisation schemes.

for both schemes. We may suggest that higher-order pomeron exchanges become less significant at higher energies depending on their nature.

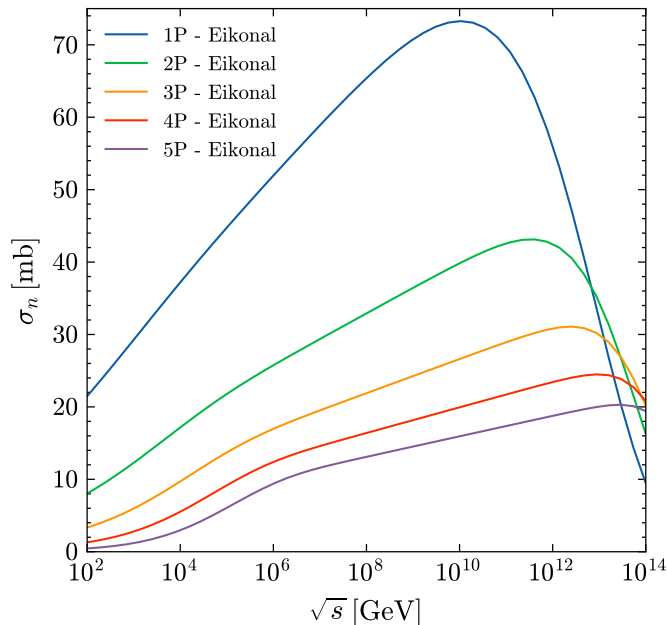


FIG. 3. Energy evolution of the Pomeron topological cross-section in the Eikonal case.

The energy evolution of the pomeron topological cross-sections for 1, 2, 3, 4 and 5-pomerons exchanged has also been examined in both the eikonal and  $U$ -matrix cases. By looking at Fig. 3 and Fig. 4, we can generally see that these cross-sections roughly exhibit the same behavior in both schemes. To be more specific, for each pomeron exchanged, the cross-sections increase as energy rises, with the contribution of 1-pomeron exchanged showing the highest value across all energy ranges. This suggests that the interactions are primarily governed by the simplest diagrams in the pomeron exchange framework, especially at lower energies. As for the higher-order pomeron exchanges ( $\sigma_{2pom}$ ,  $\sigma_{3pom}$ , etc.), they contribute gradually less. It also shows that all cross-sections tend to reach a maximum then decline abruptly at extreme energies, indicating a signature of the unitarity constraint. It is significant to note that in comparison with the eikonal case, this unitarity constraint signature is hit at a slightly higher energy for each pomeron exchanged in the  $U$ -matrix case. Indeed, this demonstrates the different energy levels at which unitarity effects take

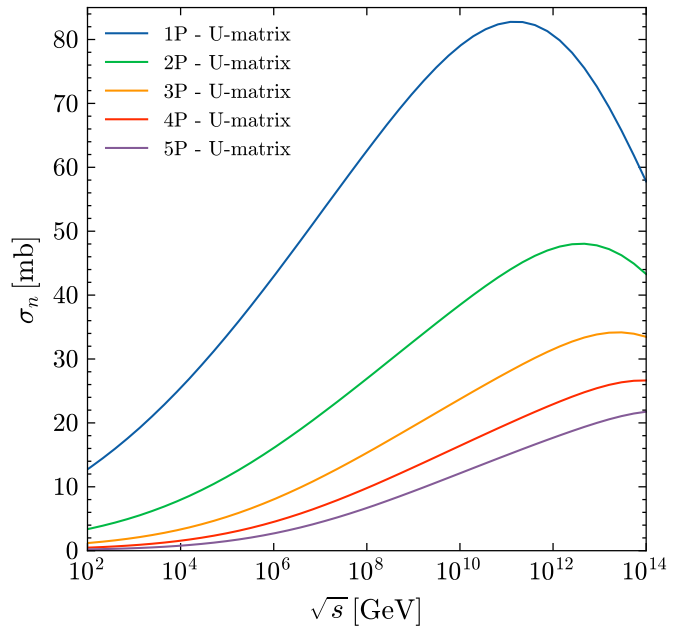


FIG. 4. Energy evolution of the Pomeron topological cross-section in the  $U$  Matrix case.

over for each pomeron contribution in these two schemes.

Furthermore, before reaching the energy threshold of the unitarity signature, it is evident that all cross-sections' curvatures, starting from 2 pomerons exchanged, significantly change at energies beyond  $10^4$  GeV in the eikonal case. It should be noted that with more pomerons being exchanged, this effect intensifies. Conversely, in the  $U$ -matrix case, despite taking into consideration several pomeron exchanges, the cross-sections show a more constant and progressive behaviour without any change in curvature.

The pomeron multiplicity distribution  $W_n(s)$ , i.e., the probability of  $n$  pomerons exchanged in an inelastic collision at the energy  $s$ , is given by

$$W_n = \frac{\sigma_n}{\sum_{n'} \sigma_{n'}} \quad (52)$$

Using the ansatz for the single pomeron exchange amplitude in the eikonal and  $U$ -Matrix cases, we compute  $W_n$ . The results are plotted in Fig. 5 for three collision energy scales.

Fig. 5 clearly shows that in the eikonal case, the exchange of a large number of pomerons is significantly suppressed compared to the  $U$ -matrix case. In the latter

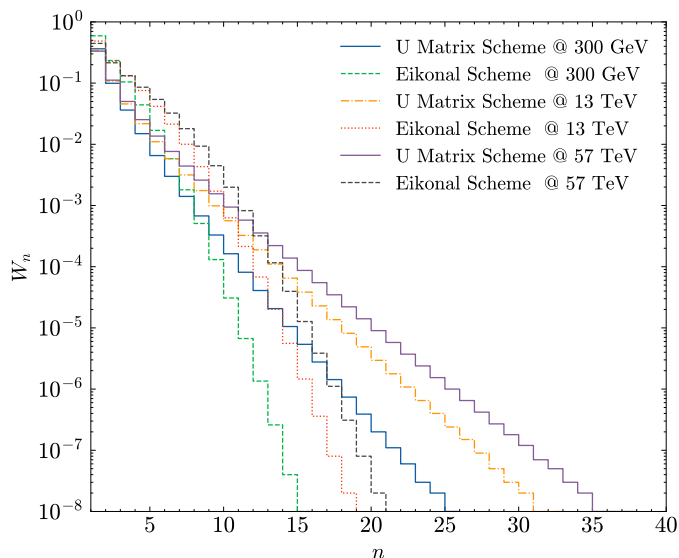


FIG. 5. Pomeron multiplicity distribution in both cases, eikonal and  $U$ -matrix.

scheme, the exchange of one pomeron enhances the probability of exchanging additional pomerons, and then the pomeron multiplicity distribution would deviate from a Poissonian one. This remarkable difference entails that multi-pomeron exchange is different in the two schemes. In particular, it may result from the presence of collective phenomena, such as correlations between the exchanged pomerons in contrast to what would be expected from an independent exchange.

It goes without saying that the role of the multi-pomeron exchange becomes more significant as energy grows. In the case of a Poisson distribution, the mean and the variance are equal. In hadronic interactions, however, their relationship tends to vary depending on a number of factors, such as the energy of the interaction. As a matter of fact, in order to highlight the role of the multi-pomeron exchange, particularly at high energy, we investigated the energy evolution of the mean and the variance of the number of pomerons exchanged. Using the probabilities in each scheme, we can calculate the mean and variance of the number of cut-pomerons as a function of the energy:

$$\langle n \rangle = \sum_{n'=0}^{\infty} n' W_{n'} \quad (53)$$

and

$$\text{Var}(n) = \sum_{n'=0}^{\infty} n'^2 W_{n'} - \langle n \rangle^2. \quad (54)$$

By looking at Fig. 6, we can clearly see that in the eikonal case both the mean and the variance of the exchanged pomerons increase more considerably with energy. In addition, it is evident that the mean-variance

relationship shows a noticeable shift around  $10^4$  GeV. More precisely, at energies below  $10^4$  GeV, we can notice that the variance is steadily smaller than the mean. This suggests that the fluctuations of the exchanged pomerons are not as severe as they are in the average behavior. This also points to a more consistent and stable interaction dynamics at lower energy, where more predictable contributions govern the pomeron exchanges. Nevertheless, at energies above  $10^4$  GeV, the variance exceeds the mean with a disproportionate growth.

It is significant to note that the result regarding the energy evolution of both the mean and the variance of the pomerons exchanged aligns with that reported in the quasi-eikonal framework [25]. Most importantly, they uncover a significant distinction in the energy shift of the mean-variance relationship. Indeed, the transition in the quasi-eikonal case, where the variance exceeds the mean, takes place at a lower energy scale, around 200 GeV. In contrast, this transition is seen at a greater energy, roughly  $10^4$  GeV, in the eikonal case. One of the possible explanations for this discrepancy is linked to the fact that the quasi-eikonal unitarization is an extended eikonal-like scheme, with an extra factor  $c$  in the expression of this unitarisation scheme accounting for the modification of the simple eikonal due to inelastic diffractive states. For instance, a value of  $c = 1.5$  is utilized, corresponding to a 50% contribution of low-mass diffractive states, in comparison to the elastic ones. Hence, the additional dynamics from the diffractive process in the quasi-eikonal scheme make the number of exchanged pomerons more variable, which lowers the energy threshold for the transition regime in which the variance is greater than the mean.

Fig. 7 demonstrates the evolution of both the mean and the variance with energy in the  $U$ -matrix scheme. As can be seen, the mean number of pomerons exchanged progressively rises as energy grows and it keeps increasing at higher energies.

As far as the variance is concerned, it exhibits a similar increase. However, surprisingly enough, it is constantly greater than the mean throughout the whole energy range. This suggests that the number of pomerons exchanged shows greater fluctuations than the average at each energy level, and this deviation becomes more significant as energy rises. As a matter of fact, this striking result can be explained in terms of the vertices, i.e., the pomeron weights, pertaining to hadronic interactions at high energy. More precisely, on the one hand, we can infer that the  $U$ -matrix scheme intrinsically incorporates diffraction production into the multi-pomeron vertices, as they are weighted by the probabilities of the fast hadron being in various diffractive states (13), reflecting a wider range of interaction possibilities. The eikonal scheme, on the other hand, having a simpler vertex structure (20) has restricted variability at lower energies and exhibits fluctuations that only exceed the mean at higher energies, where the role of the multi-pomeron exchanges becomes substantial.

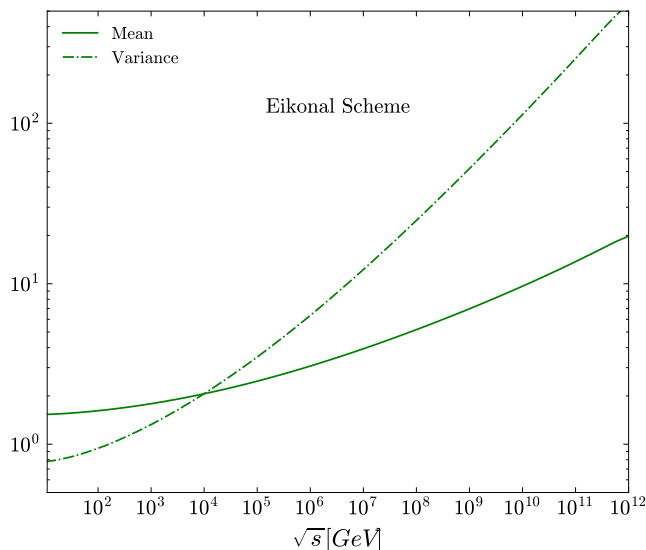


FIG. 6. Mean and variance of the number of pomerons in the eikonal and  $U$  Matrix case

Due to the fact that the  $U$ -matrix scheme yields larger fluctuations of the number of pomerons exchanged irrespective of the energy range in comparison to the simpler eikonal and the quasi-eikonal schemes, we can argue that it accounts for more complex interaction dynamics and for a larger amount of diffraction production. Interestingly, this resonates with a result obtained in [13] and most importantly helps explain why the  $U$ -matrix scheme describes the single diffractive data slightly better than the eikonal regardless of the data employed.

The disparity between the  $U$ -matrix and eikonal frameworks, with respect to the fluctuations in the number of pomerons exchanged, is most likely due to the diffractive states' overlap. It is significant to note that, the difference between the two schemes with regards to the parametrized hadronic overlap function is marginal (48). However, in the  $U$ -matrix scheme, there is a considerable diffractive states' overlap, which increases pomerons' variability and gives rise to more pronounced fluctuations. Conversely, since the eikonal scheme does not take into consideration such overlap, it shows simpler dynamics with suppressed fluctuations at lower energies. This comparison sheds light on the role that the  $U$ -matrix scheme plays in accounting for more intricate dynamics, particularly, when considering scattering processes with significant diffractive contributions.

Overall, despite the marginal difference in the functional form of the pomeron input in both schemes, we can deduce that the mechanism of unitarization significantly affects the fluctuations in the number of pomerons exchanged, and claim that the  $U$ -matrix scheme offers an efficient phenomenological approach to consider pomerons' variability regardless of the energy range, while such fluctuations become significant only beyond specific high-energy thresholds in the other schemes, namely the

eikonal and quasi-eikonal.

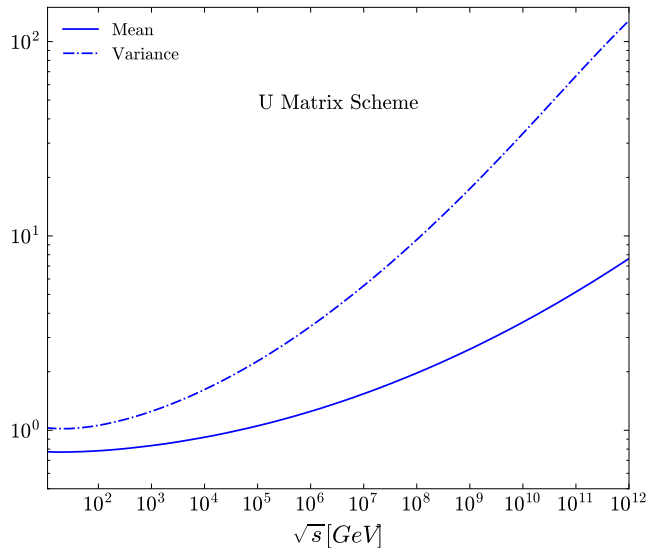


FIG. 7. Mean and variance of the number of pomerons in the eikonal and  $U$  Matrix case

The intriguing energy shift with regards to the mean-variance relationship hints at a transition in the underlying dynamics of the hadronic scattering process with respect to the energy regime. Thus, in order to better comprehend this energy transition, we will examine the  $f_2$  moment of the pomeron multiplicity distribution, i.e., the two-particle correlation parameter, measuring the correlation between pairs of pomerons, across various energies within both the eikonal and  $U$ -matrix frameworks. This parameter is defined as follows :

$$f_2 = \langle n(n-1) \rangle - \langle n \rangle^2 = D_2^2 - \langle n \rangle \quad (55)$$

where  $D_2$  is the dispersion:  $D_2^2 = \langle n^2 \rangle - \langle n \rangle^2$ . The two-particle correlation parameter has three possible values: negative, zero, and positive, in accordance with the multiplicity distributions that are narrower, equal to, or broader than a Poisson distribution.

By looking at Fig. 8, we can vividly see in the eikonal case that the  $f_2$  moment displays a changing behavior in variation with energy. Indeed, at energies below  $10^4$  GeV, the  $f_2$  moment is negative. This suggests that the pomeron multiplicity distribution is narrower than the Poisson distribution. This also implies that the particle production fluctuations are suppressed and the number of pomeron exchanges is distributed uniformly. At  $10^4$  GeV, the value of the  $f_2$  moment is zero, which is indicative of the alignment of both the pomeron multiplicity and the Poisson distributions. This entails independent and randomly occurring events. At energies above  $10^4$  GeV, the  $f_2$  moment becomes positive. This demonstrates that the pomeron multiplicity distribution is broader than the Poisson distribution, indicating an enhancement of pomeron fluctuations.

Turning now to the  $U$ -matrix case, Fig. 8 strikingly shows that the  $f_2$  moment remains positive throughout various energy ranges, suggesting that the pomeron multiplicity distribution is constantly broader than the Poisson distribution and hence indicating an enhancement of pomeron fluctuations. These fluctuations become more noticeable with increasing energy and are remarkably constantly larger than those yielded in the eikonal case.

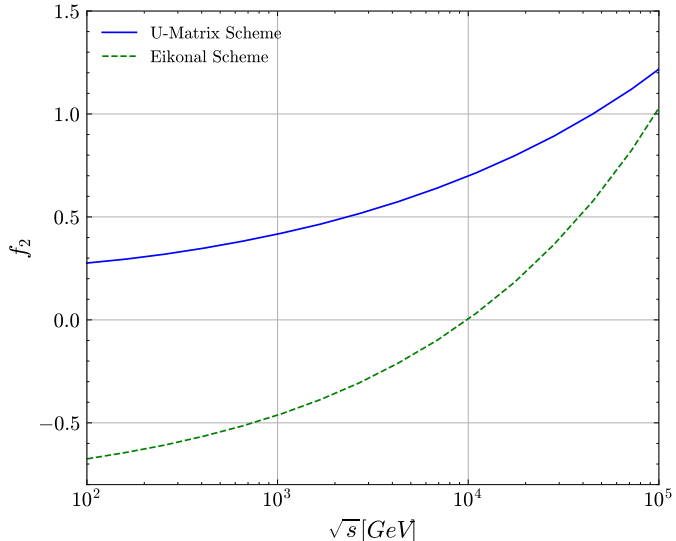


FIG. 8. The two-particle correlation parameter versus the interaction energy in the eikonal and  $U$  Matrix case

Fig. 9 displays the behavior of the  $f_2$  parameter with respect to the mean number of pomerons in the eikonal and  $U$ -matrix cases, specifically for energies exceeding  $10^4$  GeV, where both schemes manifest pomeron fluctuations. It is apparent from this figure that both schemes yield amplified fluctuations. It also shows that the increasing mean number of pomerons with energy results in a rise in the correlation between pairs of pomerons. Nevertheless, it is worth noting that when comparing the two schemes, the correlation between pairs of pomerons rises considerably faster as the number of exchanged pomerons increases in the  $U$ -matrix scheme. This signifies that this latter incorporates enhanced correlations, indicating strong multi-pomeron dynamics.

It is evident from the sharper increase in  $f_2$  in the  $U$ -matrix case that the two approaches handle high-energy hadronic interactions differently, with the  $U$ -matrix revealing more noticeable pomeron collective effects and non-linear pomeron exchanges.

These results strongly confirm our previous assertion that the  $U$ -matrix scheme naturally comprises pomeron statistical fluctuations that are distinct from those in eikonal-like schemes and further explain their impact on the properties of hadronic multi-particle production, in particular the unexpected overestimation of the fluctuations and correlations between final state particles with increasing energy in  $pp$  collisions, as shown in [8].

In view of the aforementioned results, we understand that the energy transition in the underpinning dynamics of the scattering process, which is only present in eikonal-like schemes, stems from a movement from a regime of suppressed pomeron fluctuations to a regime of enhanced fluctuations with increasing energy.

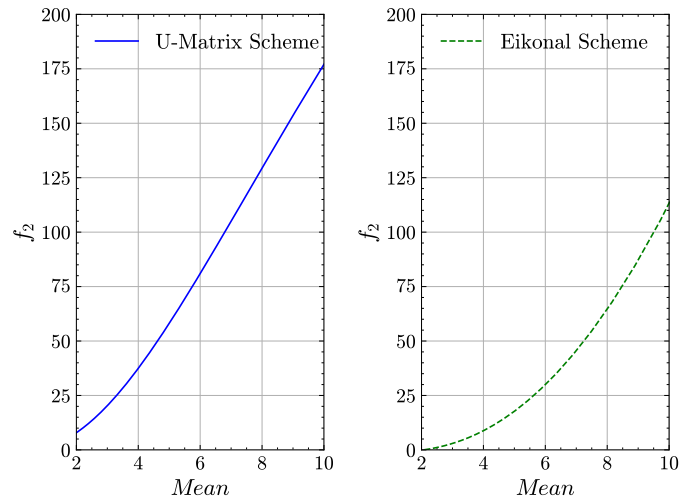


FIG. 9. The two-pomeron correlation parameter versus the average pomeron in the eikonal and  $U$  Matrix case

In light of the presence of enhanced pomeron fluctuations and a broader distribution within the  $U$ -matrix scheme, it is argued that the exchanged pomerons exhibit correlations which could be the result of collective effects, such as those stemming from the overlap of diffractive states that are in turn, emerging from the pomeron weights.

In an attempt to better comprehend these correlations, the higher-order moments of the pomeron multiplicity distribution were analyzed, as will be seen in the forthcoming subsection.

### C. Pomeron correlations

In order to elucidate the nature of correlations among the pomerons exchanged in hadronic collisions, we examine the normalized factorial moments  $F_q$  of the pomeron multiplicity distribution. In fact, the moment  $F_q$  equals unity for all rank  $q$  in the case of an independent exchange of pomerons. Nevertheless,  $F_q$  is greater (less) than unity depending on whether the exchanged pomerons are correlated (anti-correlated) [26]. These moments are provided by

$$F_q = \frac{1}{\langle n \rangle^q} \sum_{n=q}^{\infty} n(n-1)\dots(n-q+1) P_n, \quad (56)$$

where  $\langle n \rangle = \sum_n n W_n$  is the average multiplicity and  $q$  is the rank of the moment. In the eikonal case, regard-

less of the energy scale, the normalized factorial moment remains equal to 1 for all ranks  $q$ , reflecting a Poisson distribution of the exchanged pomerons and indicating an uncorrelated distribution of events. In case of the  $U$ -matrix scheme, the moments are given by :

$$E(X^q) = p \text{Li}_{-q}(1-p) \quad (57)$$

where  $\text{Li}_{-q}(1-p)$  is the polylogarithm function. So the normalized factorial moment of rank  $q$  is given by :

$$F_q(s) = \frac{p \text{Li}_{-q}(1-p)}{\left(\frac{1-p}{p}\right)^q} \quad (58)$$

and  $p$  defined by 36.

Fig. 10 illustrates the behavior of the normalized factorial moments of pomerons exchanged in function of the rank  $q$  of pomerons and across various impact parameter  $b$  values within the framework of the  $U$ -matrix scheme, specifically at 13 GeV and 57 GeV. According to this figure, we can see that the normalized factorial moments  $F_q$  exhibit a considerably increasing pattern with  $q$  at both energies, indicating stronger higher-order correlations, where pomeron correlations emerge from  $q = 3$  at 13 GeV, with two pomerons showing anti-correlation. However, they appear starting from  $q = 2$  at 57 GeV, with all pomerons being positively correlated.

In both energies, when  $b = 0$  fm,  $F_q$  is the highest suggesting that the strongest correlations occur in central collisions. Nevertheless, when  $b$  rises, we observe a decrease in  $F_q$ , indicating weaker correlations in less-central collisions because of a reduced interaction overlap. When comparing the two energies,  $F_q$  values are consistently greater at 57 GeV than at 13 GeV for all pomerons exchanged and impact parameter  $b$ , showing that pomeron correlations become more intense as center-of-mass energy increases. In addition, at both energies,  $F_q$  remains dependent on  $b$ , with correlations decreasing as  $b$  rises. Yet, it is significant to note that at 57 GeV we have stronger correlations even at larger  $b$ . This highlights that increasing collision energy mediates the influence of the impact parameter on the correlation strength while simultaneously strengthening correlations and reducing the prevalence of anti-correlation effects.

On the whole, both the energy and the impact parameter  $b$  have a combined impact on the correlation between pomerons exchanged, indicating that these two parameters are not entirely independent when it comes to influencing the number of elementary interactions.

To delve deeper in the interdependence between these two factors, we demonstrate in Fig. 11, 12, 13 and 14 the impact parameter evolution of the normalised factorial moment for various energy scales and different pomerons exchanged. One intriguing trend revealed by this evolution is that for each energy,  $F_q$  shows an inflection point at a specific value of  $b$  at which the correlation strength changes noticeably. Moreover, we can see that as energy

increases, this inflection point moves to larger impact parameters, implying that the correlations between exchanged pomerons spread out more in transverse space. And, at extremely high energies, it reaches a value of about 1 fm, where correlations are roughly zero. In this regard, we suggest that as energy grows, the spatial scope of the interactions becomes more significant, reflecting an interdependence between the energy scale and the transverse position of pomerons.

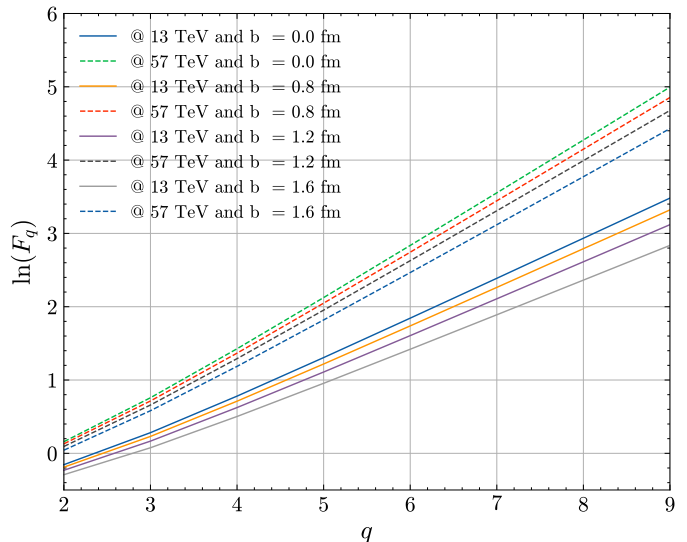


FIG. 10. Normalized factorial moment of pomeron exchanges as a function of the rank  $q$  and for different impact parameter  $b$  values with the  $U$  Matrix scheme

As a matter of fact, the aforementioned findings come in support of a previous suggestion that the  $U$ -matrix unitarization is probably incompatible with uncorrelated pomeron exchanges as there was no improvement in the description of the single diffractive data with a multi-channel model compared to a two-channel one [9]. To be more specific, [9] a multi-channel model of high-energy hadron interactions was created by considering a full parton configuration space and using the  $U$ -matrix unitarization scheme. Moreover, the mean number of interactions between partons was assumed to be expressed as a product of the single-pomeron scattering amplitude, together with functions of the impact parameter and configurations. Furthermore, we assumed that the impact parameter had no effect on the distribution of parton configurations. Nevertheless, in the present study, the interdependence effect observed between  $s$  and  $b$  on the number of pomerons exchanged breaks down the rigorous validity of such factorization within the  $U$ -matrix scheme. Furthermore, aside from its ease of use as a workable framework, as with the eikonal approach, this factorization assumption is short of a compelling theoretical foundation. As a result, the parton distribution functions cannot be efficiently separated into longitudinal and transverse components.

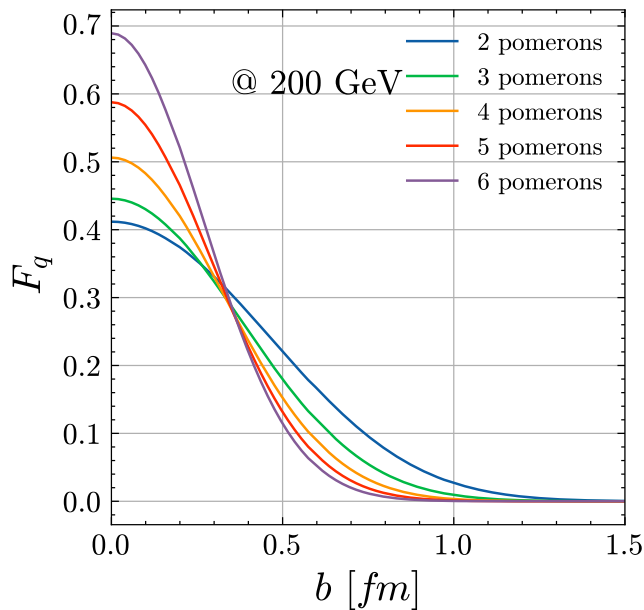


FIG. 11. Impact parameter evolution of the normalized factorial moment at 200 GeV

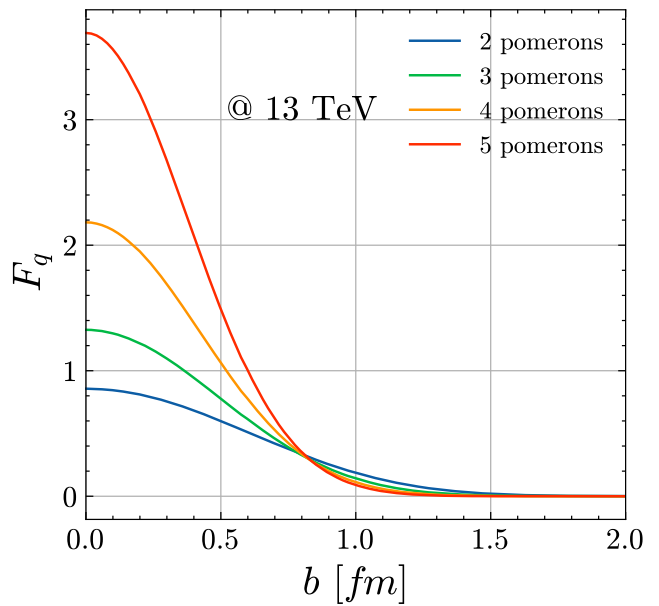


FIG. 13. Impact parameter evolution of the normalized factorial moment at 13 TeV

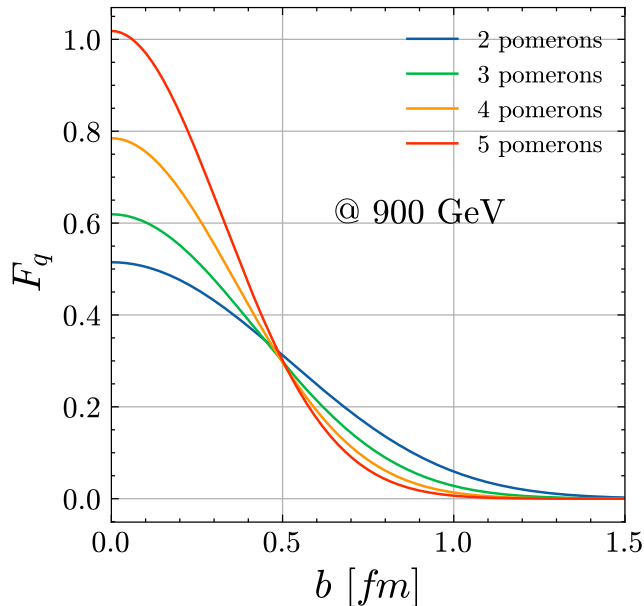


FIG. 12. Impact parameter evolution of the normalized factorial moment at 900 GeV

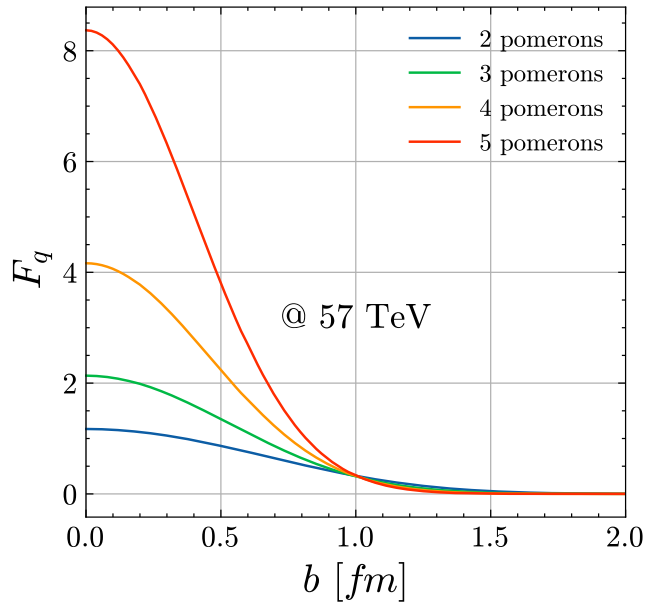


FIG. 14. Impact parameter evolution of the normalized factorial moment at 57 TeV

We can contend that the  $U$ -matrix approach offers a more suitable framework, as it provides a more accurate representation of the underlying elementary interactions, by taking into account the interdependence on all hadronic degrees of freedom. Moreover, correlations between pomerons allow the hadron's internal partonic structure to evolve dynamically during the scattering process. Thus, the  $U$ -matrix scheme does not require the hadrons to be frozen in their internal partonic

configurations during the interaction, unlike the eikonal. Furthermore, by allowing for correlation between the exchanged pomerons, one can take into account the fact that the first pair of quark-antiquark strings is different from subsequent pairs, as the pomeron weights influence the dynamics of string pair formation. Consequently, the inconsistencies between the string model and the Gribov-Regge theory in hadronization models could be partially resolved within the  $U$ -matrix scheme.

#### D. Multiplicities in pp collisions

Correlations between partons are known to occur as a result of the fundamental dynamics of partonic interactions as well as the spatial and momentum structure of the hadron. In fact, these correlations are critical in identifying the topological cross-sections for processes, such as double and triple parton scattering, which in turn influence the observed multiplicity patterns and cross-sections in hadronic collisions.

This subsection elucidates the role of the correlated multi-pomeron exchange in hadronic collisions by analyzing the multiplicity distribution of  $pp$  and  $\bar{p}p$  collisions from the point of view of multi-parton interactions, as described by string models along with the Regge Phenomenology (see the introduction section). According to this conjunction, a cut in the multi-pomeron exchange diagram is responsible for the hadrons yielded in the final state. More precisely, a cut of  $n$  pomerons results in  $2n$  chains that connect to the partons of the initial hadrons. The number  $n$ , representing the pairs of simultaneously colliding partons from the different hadrons involved in the interaction, corresponds to the number of resulting showers. For instance,  $n = 1$  translates into a single collision of one pair of partons emerging from the two colliding hadrons, which is ascribed to the Regge pole.  $n = 2$  corresponds to a double collision of two pairs of partons from the different hadrons, which refers to the exchange of two pomerons, and so on.

In our analysis of the cross-section corresponding to the production of  $N$  secondary hadrons,  $\sigma_N(s)$ , diffraction processes were not considered so as to overlook long-distance correlations among particles within the same shower and the picture of the hadronic multi-particle production based on the Dual Parton Model (DPM) presented in [27] was followed mainly for comparison purposes.

In fact, in order to simplify our analysis, we assumed that the multiplicity distribution maintains its Poissonian character regardless of the energy scale, in spite of the known phenomenon of the violation of the KNO scaling [28] which entails that as energy increases, the hadronic multiplicity distribution broadens and deviates from a purely Poissonian nature :

$$P_n(N) = \frac{\langle N_n \rangle^N}{N!} e^{-\langle N_n \rangle} \quad (59)$$

where  $\langle N_n \rangle$  represents the mean number of particles produced in  $n$  showers and is taken proportional to the mean multiplicity for a single shower :

$$\langle N_n \rangle = n \langle N_1 \rangle \quad (60)$$

and the mean multiplicity for a single shower is modelled as :

$$\langle N_1 \rangle = a + b \ln(s/s_0) \quad (61)$$

representing a logarithmic growth with centre-of-mass energy  $s$ , in agreement with experimental observations at low energy, with  $a = -7.3$  and  $b = 2.56$  from [27]. Thus, the total inelastic cross-section is constructed as a sum over contributions from  $n$ -shower events:

$$\sigma_{in}(N, s) = \sigma_1 P_1(N) + \sigma_2 (P_2(N) + \sigma_3 P_3(N) + \dots), \quad (62)$$

where the pomerons weights  $\sigma_n(\xi_n)$  are given after impact parameter integration of the cross-section for the production of  $n$  showers in both schemes (32), (29) and  $\xi_n = \ln\left(\frac{s}{s_0 n^2}\right)$ . We retain three terms in 62 since the quadruple (or four-parton pair) collision has a small effect.

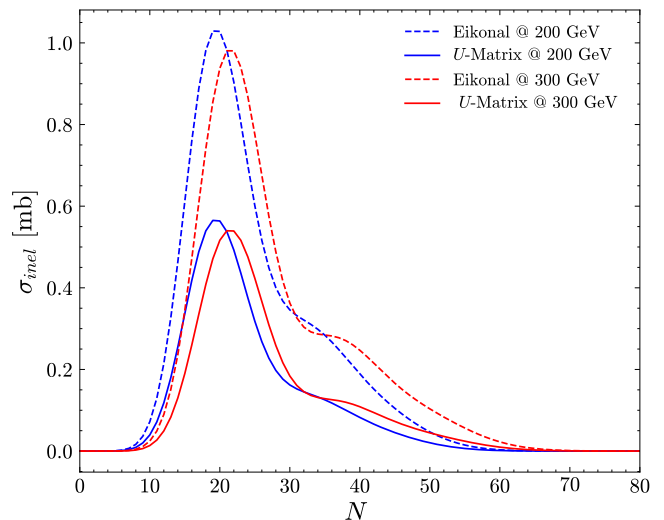


FIG. 15. Topological cross sections  $\sigma_N$  in the eikonal and  $U$  Matrix approximation with exchanges of three effective soft Pomeron.

By looking at Fig. 15 and Fig. 16, the shoulder, associated with the double collision, is clearly visible at low energies in the eikonal case, which is in concordance with the quasi-eikonal case [27]. Interestingly enough, in the  $U$ -matrix case, this second peak of  $\sigma_N(s)$  is rather slightly resolved and tends to become broader and lower with increasing energy as opposed to the eikonal case. This behavior can be explained by the impact of correlated pomeron exchanges given that parton correlations enhance the probability of multi-parton collisions and hence re-distribute the contributions throughout the topological cross-sections. Thus, in the  $U$ -matrix scheme, correlated pomeron exchanges play a key role in enhancing multi-parton collisions, particularly double parton collisions.

These outcomes suggest that pomeron exchanges in the  $U$ -matrix framework embed a probability of concurrently finding partons with momentum fractions  $x_1$  and  $x_2$  within the hadron, which is represented by a non-zero correlation function  $F(x_1, x_2)$ , emphasizing the deviation

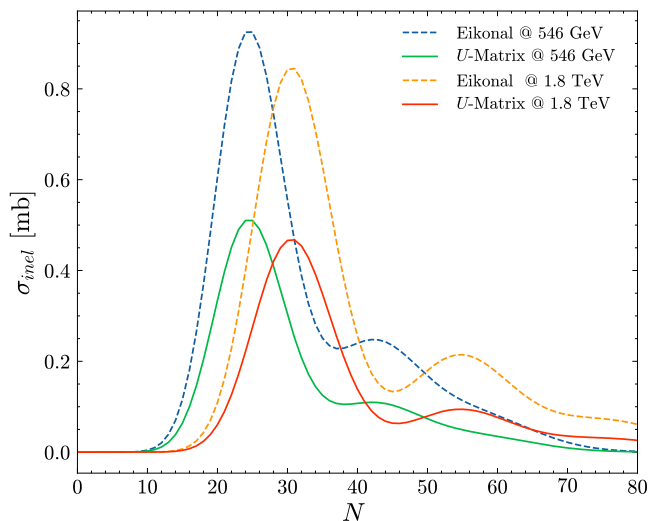


FIG. 16. Topological cross sections  $\sigma_N$  in the eikonal and  $U$  Matrix approximation with exchanges of three effective soft Pomerons.

from independent multi-parton interactions. In this regard, one may wonder how the  $U$ -matrix approach could allow disentangling correlations in multiple parton interactions, specifically separating the effects of fractional momentum correlations from those of transverse coordinate correlations, which is beyond the remit of this paper.

It is worth noting that in [27], the Dual Parton Model (DPM) was used to describe the double-parton collision, while solely taking the soft pomeron as the main component mediating the interactions between partons and comparing it to its hard counterpart. It has been argued that soft interactions are also responsible for the double inelastic parton collisions, which is confirmed by our result.

Moreover, given that the DPM is based on the quasi-eikonal scheme, we can infer that the incorporation of higher levels of diffractive production, resulting in an enhanced parton correlation, makes the  $U$ -matrix scheme a more reliable approach to the description of multi-parton collisions, compared to both the eikonal and quasi-eikonal schemes.

Owing that the soft interactions are also responsible for the double parton collisions, while a cut pomeron comprises contributions from both hard and soft processes, this makes us wonder about its nature, particularly in relation to the hard-soft hadronic physics transition, and may pave the way for a unified description of high-energy hadronic collisions in the context of the  $U$ -matrix.

#### IV. CONCLUSION

The chief purpose of the present paper was to understand the nature of the pomeron exchanges in hadronic interaction. Using a generalized representation of the

unitarized hadronic elastic amplitude, the pomeron topological cross section was derived for both the  $U$ -matrix and eikonal schemes. Our results have demonstrated that the mechanism of the multi-pomeron exchange summation is distinct in each scheme at many levels. To be more specific, it has been found that in the impact parameter space, the elementary interactions tend to occur at the core of the collision in the  $U$ -matrix case as opposed to the eikonal case.

In addition, in both schemes, it has been shown that the pomeron topological cross-section for each higher-order exchanged pomeron increases with increasing energy and tends to reach a maximum then suddenly decreases at extreme energies, which marks the unitarity constraint. However, this unitarity constraint mark is reached at a somewhat higher energy for each pomeron exchanged in the  $U$ -matrix case. The disparity between the two schemes has also been shown concerning the curvature of this cross-section. More specifically, in the eikonal case, it considerably changed at energies beyond  $10^4$  GeV. In the  $U$ -matrix case, no change was observed.

Furthermore, the pomeron multiplicity distribution has been computed. In the  $U$ -matrix case, the pomeron exchange is a random variable geometrically distributed, and the exchange of one pomeron has been demonstrated to enhance the probability of exchanging additional pomerons.

Moreover, in the  $U$ -matrix case, the number of pomerons exchanged has shown greater fluctuations than the average at each energy level, and this deviation becomes more significant as energy rises. It has been deduced that the  $U$ -matrix scheme intrinsically incorporates diffraction production into the multi-pomeron vertices, reflecting a larger pomerons' variability regardless of the energy range, while such fluctuations become significant only beyond a specific high-energy threshold in the eikonal and quasi-eikonal schemes.

Furthermore, the pomeron exchange in the  $U$ -matrix scheme exhibits collective effects, as an increase in the number of exchanged pomerons leads to more pronounced higher-order pomeron correlations, which depend on both the energy and the impact parameter. This behavior contrasts with the independent pomeron exchange characteristic of the eikonal scheme.

Last but not least, the impact of pomeron weights on the proton-proton multiplicity distribution has been examined from the point of view of multi-parton interactions. The results have revealed that, in the  $U$ -matrix scheme, correlated pomeron exchanges play a key role in enhancing multi-parton collisions, particularly double parton collisions.

We understand from the findings of this study that the pomeron distribution is fixed by the unitarization scheme chosen to satisfy the unitarity constraint, and that this choice cannot be arbitrary.

In light of these results, although there is no fundamental theory to compute the vertices in hadronic interactions at high energy, we can claim that the  $U$ -matrix



scheme may incorporate the proper vertices for such phenomena. We also argue that the distribution of the number of elementary interactions pertaining to the  $U$ -matrix scheme should be implemented in Monte Carlo event generator in order to have more realistic predictions for high and ultra-high energy hadronic observables.

## ACKNOWLEDGMENTS

RO would like to thank Jean-René Cudell for his invaluable comments. RO also appreciates the insightful discussions with Sergey Troshin. Special thanks go to the computational resource provided by Consortium des Équipements de Calcul Intensif (CÉCI), funded by the Fonds de la Recherche Scientifique de Belgique (F.R.S.-FNRS) where a part of the computational work was carried out.

- 
- [1] B. Andersson, G. Gustafson, G. Ingelman, and T. Sjöstrand, *Physics Reports* **97**, 31 (1983).
  - [2] V. N. Gribov, *Zh. Eksp. Teor. Fiz.* **53**, 654 (1967).
  - [3] F. Riehn, R. Engel, A. Fedynitch, T. K. Gaisser, and T. Stanev, *Phys. Rev. D* **102**, 063002 (2020).
  - [4] S. Ostapchenko, *EPJ Web Conf.* **208**, 11001 (2019).
  - [5] K. G. Boreskov, A. B. Kaidalov, V. A. Khoze, A. D. Martin, and M. G. Ryskin, *The European Physical Journal C* **44**, 523–531 (2005).
  - [6] E. Martynov and G. Tersimonov, *Phys. Rev. D* **101**, 114003 (2020).
  - [7] F. M. Liu, J. Aichelin, M. Bleicher, H. J. Drescher, S. Ostapchenko, T. Pierog, and K. Werner, *Phys. Rev. D* **67**, 034011 (2003).
  - [8] R. Oueslati and A. Trabelsi, *JHEP* **07**, 100, [arXiv:2403.02263 \[hep-ph\]](https://arxiv.org/abs/2403.02263).
  - [9] R. Oueslati, *JHEP* **08**, 087, [arXiv:2305.03424 \[hep-ph\]](https://arxiv.org/abs/2305.03424).
  - [10] R. Blankenbecler and M. L. Goldberger, *Phys. Rev.* **126**, 766 (1962).
  - [11] S. M. Troshin and N. E. Tyurin, *Journal of Physics G: Nuclear and Particle Physics* **29**, 1061 (2003).
  - [12] K. Ohashi, H. Menjo, Y. Itow, T. Sako, and K. Kasahara, *Progress of Theoretical and Experimental Physics* **2021**, 033F01 (2021), <https://academic.oup.com/ptep/article-pdf/2021/3/033F01/36647718/ptab013.pdf>.
  - [13] A. Vanthieghem, A. Bhattacharya, R. Oueslati, and J.-R. Cudell, *JHEP* **09**, 005, [arXiv:2104.12923 \[hep-ph\]](https://arxiv.org/abs/2104.12923).
  - [14] G. Feofilov, V. Kovalenko, and A. Puchkov, *EPJ Web Conf.* **171**, 18003 (2018), [arXiv:1711.00842 \[nucl-th\]](https://arxiv.org/abs/1711.00842).
  - [15] J. Bleibel, L. V. Bravina, A. B. Kaidalov, and E. E. Zabrodin, *Phys. Rev. D* **93**, 114012 (2016), [arXiv:1011.2703 \[hep-ph\]](https://arxiv.org/abs/1011.2703).
  - [16] O. V. Kancheli, (2013), [arXiv:1309.5860 \[hep-ph\]](https://arxiv.org/abs/1309.5860).
  - [17] V. N. Gribov, *Soviet Physics JETP* **100** (1983).
  - [18] V. N. Gribov and A. A. Migdal, *Sov. J. Nucl. Phys.* **8**, 1002 (1968).
  - [19] J.-R. Cudell, E. Predazzi, and O. V. Selyugin, *Phys. Rev. D* **79**, 034033 (2009), [arXiv:0812.0735 \[hep-ph\]](https://arxiv.org/abs/0812.0735).
  - [20] There appears to be a typo in the formula in [16].
  - [21] N. L. Johnson, S. Kotz, and A. W. Kemp, *Univariate Discrete Distributions*, 2nd ed. (John Wiley & Sons, New York, 1992).
  - [22] E. G. S. Luna and M. G. Ryskin, *Phys. Rev. D* **110**, 094007 (2024), [arXiv:2408.00194 \[hep-ph\]](https://arxiv.org/abs/2408.00194).
  - [23] There appears to be a typo in the formula in [16].
  - [24] A. Bhattacharya, J.-R. Cudell, R. Oueslati, and A. Vanthieghem, *Phys. Rev. D* **103**, L051502 (2021), [arXiv:2012.07970 \[hep-ph\]](https://arxiv.org/abs/2012.07970).
  - [25] E. Bodnia, D. Derkach, G. Feofilov, V. Kovalenko, and A. Puchkov, *PoS QFTHEP2013*, 060 (2013), [arXiv:1310.1627 \[hep-ph\]](https://arxiv.org/abs/1310.1627).
  - [26] I. M. Dremin, *Phys. Usp.* **37**, 715 (1994), [arXiv:hep-ph/9406231](https://arxiv.org/abs/hep-ph/9406231).
  - [27] S. G. Matinyan and W. D. Walker, *Phys. Rev. D* **59**, 034022 (1999), [arXiv:hep-ph/9801219](https://arxiv.org/abs/hep-ph/9801219).
  - [28] Z. Koba, H. Nielsen, and P. Olesen, *Nuclear Physics B* **40**, 317 (1972).